Tellus (1995), 47A, 162–174
Printed in Belgium – all rights reserved

TELLUS
ISSN 0280–6495

Numerical experiments on the genesis of Sharav cyclones: idealized simulations

By JOSEPH EGGER[1]*, PINHAS ALPERT[2], ARNOLD TAFFERNER[1] and BARUCH ZIV[2],
[1]*Meteorologisches Institut der Universität München, Theresienstrasse 37, 80333 München, Germany*;
[2]*Department of Geophysics and Planetary Sciences, Tel Aviv University, 69978 Tel Aviv, Israel*

(Manuscript received 2 December 1993; in final form 16 June 1994)

ABSTRACT

A three-level channel flow model is used to investigate the generation of Sharav cyclones in the lee of the Atlas mountains through "idealized" numerical experimentation. A typical initial state consists of a barotropic high–low system, embedded in baroclinic shear flow and centered to the north of the Atlas mountains. If this "perturbation" is of sufficient strength, a cold-air outbreak occurs in the rear of the low as well as a southward excursion of the trough at upper levels. The cold air is blocked by the Atlas mountains, if the initial location of the low is chosen properly. The upper-level trough intensifies slightly when crossing the mountain range and induces then a low-level cyclone in the lee. The trough turns eastward later on and the new cyclone is staying close to this upper-level centre. A simple two-dimensional three-layer model is used to explain salient features of this type of lee cyclogenesis. Moreover, additional experiments are conducted in order to elucidate details of the cyclogenetic process.

1. Introduction

Sharav cyclones, sometimes referred to as "Saharan depressions" or "Khamsin depressions" form in the lee of the Atlas mountains, either when a north–westerly air stream moves over the Atlantic towards the Atlas range or when a north–easterly wind is blowing over the western Mediterranean towards these mountains (Weather in the Mediterranean, 1962). They form most frequently in spring (e.g., Alpert and Ziv, 1989; referred to as AZ). "Saharan depressions may develop and move quickly eastwards if a good supply of arctic or polar air is maintained. Otherwise they may remain almost stationary for days, but on the whole slow development is more common than rapid development and movement" (Weather in the Mediterranean, 1962). According to Alpert et al. (1990; their Fig. 2), Sharav cyclone tracks in spring are oriented east- to north-eastward. Pedgley (1972) as well as AZ point out that Sharav depressions are linked to upper level troughs to the west. AZ, in their review of Sharav cyclones, concentrate on the maturing stage of these depressions which exhibit fast motion towards the east after they left the Atlas region. Typical horizontal (vertical) scales are $\leqslant 1000$ km (3–5 km) in that stage, a standard surface pressure amplitude is ~ 10 hPa. AZ argue, that the intensification of these cyclones on their way to the Eastern Mediterranean is mainly due to the heating contrast at the North African coast in a weakly baroclinically unstable environment.

Although some Sharav cyclones appear to originate at the North African coast (AZ) and others in the southern part of the Sahara (Pedgley, 1972), we are concerned here only with those originating in the lee of the Atlas mountains. It is the purpose of this note to investigate the genesis of these Sharav cyclones, a topic which has attracted little attention in the literature. In particular, we are not aware of any related theoretical and/or numerical work. Of course, the phenomenon of

* Corresponding author.

lee cyclogenesis has attracted theoreticians since long. However, corresponding theories have been developed for cyclogenesis in the lee of the Alps (see Mesinger and Pierrehumbert 1986 for a review) or the Rocky Mountains. It is not immediately obvious if these theories can be applied to the Atlas mountains, which are situated in an area where the synoptic climatology differs from that of the Alps or that of the Rocky Mountains.

In this part of the paper, we wish to conduct "idealized" simulations in order to investigate the genesis of Sharav cyclones. In such numerical experiments, an initial state is prescribed which is thought to be typical of situations which are conducive to the generation of Sharav cyclones. We rely on the evidence presented in Weather in the Mediterranean (1962), where a strongly elongated upper-level trough or a cut-off low moves over the Atlas mountains with subsequent leeside development in all cases shown (7–8 May 1949, Figs. 2.10c, d; 14 April 1954, Figs. 2.11a, b; 7 April 1954, Figs. 2.35a, b). Indeed, cyclones can be generated in the lee of the Atlas mountains. The most important factors in this process are singled out through systematic variations of the initial state and of the topography.

2. The model

The model to be used is described in Egger (1988). It is based on the hydrostatic Boussinesq equations on the f-plane. Horizontal and vertical diffusion of momentum and heat have been added to the model equations as given in Egger (1988). The flow is confined to a channel with periodic boundary conditions in west–east (x)-direction and solid walls to the north and south. The upper boundary of the model fluid is a free surface with reduced gravity $g' = 1\ \mathrm{ms}^{-2}$. Mountains are incorporated as blocking obstacles with vertical walls. We require vanishing components of the velocity vertical to a wall. The variables are staggered (see Fig. 1 of Egger, 1988) in a grid of horizontal mesh size $\mathrm{D}x = 120$ km. There are three layers with a vertical spacing $\mathrm{D}z = 8000/3$ m. The channel's length (width) is $L = 38\ \mathrm{D}x$, ($D = 38\ \mathrm{D}x$). In addition to wind, potential temperature θ and the height η of the free surface we predict also the position I, J, K of Lagrangian tracers according to:

$$\frac{\mathrm{d}I}{\mathrm{d}t} = \frac{\mathrm{d}J}{\mathrm{d}t} = \frac{\mathrm{d}K}{\mathrm{d}t} = 0, \tag{1}$$

where

$$\frac{\mathrm{d}}{\mathrm{d}t} = \frac{\partial}{\partial t} + u\frac{\partial}{\partial x} + v\frac{\partial}{\partial y} + w\frac{\partial}{\partial z}.$$

The initial conditions at the gridpoints are $I = i$, $J = j$, $K = k$, where i, j, k are the gridpoint indices in the corresponding directions ($0 < i < 39$; $0 < j < 39$; $0 < k < 4$ in a standard run). On principle, we could have computed trajectories as well. However, it appears preferable to integrate (1) in the grid of the model since that is the way the model is handling the "conservation of particles". An upstream scheme is used when solving (1).

Obviously, our model is extremely simple and designed to capture only rather robust processes. However, this model has been found suitable for testing theories of lee cyclogenesis in Egger (1988). We expect, therefore, that this model will also be helpful in elucidating the genesis of Sharav cyclones.

3. The initial state

The set-up of the numerical experiments must contain all those features which are thought to be important in inducing the generation of a Sharav cyclone. Clearly, we need a representation of the Atlas mountains. These are incorporated in the model as an west–east orientated massiv of 1320 km length, 240 km width and a height of 2700 m blocking the flow in the lowest layer (see Fig. 1). There are at least indications that the formation of a Genoa depression may precede in some cases that of a Sharav cyclone (see Fig. 2.33 of Weather in the Mediterranean 1962 and Fig. 6 of AZ). Therefore, the Alps are also represented as an obstacle (see Fig. 1) blocking the lowest layer of the model. It is conceivable that the orography of the Iberian peninsula is playing a role as well in the formation of Sharav cyclones. However, a much more refined grid would be needed to capture such effects.

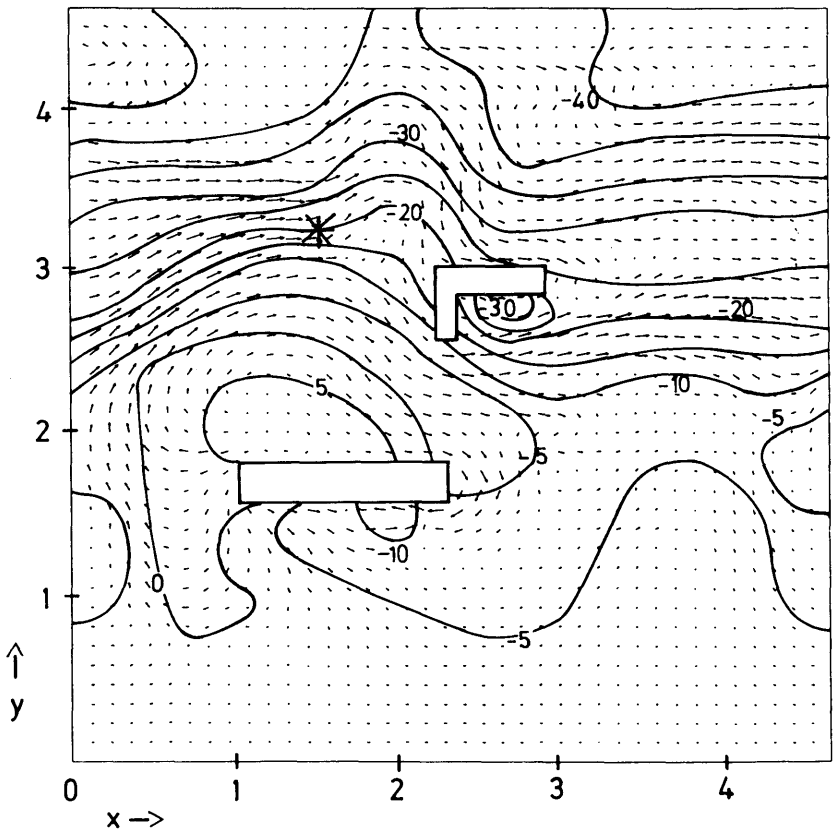

Fig. 1. Wind and deviation pressure (hPa) at $t = 60$ h in the lowest layer of the model (at geometric height $z = 1333$ m) in experiment A. The star marks the position of the center of the parent cyclone at $t = 0$ h. Maximum wind speed is 41 ms^{-1}. The shape of the Atlas mountains and of the Alps is given by the corresponding polygons. There is no flow in the lowest layer within these obstacles. Distances in 10^6 m. In this Boussinesq model pressure is defined as a deviation from a fixed mean pressure $p_0(z)$. Contour interval 5 hPa.

We create a baroclinic wave disturbance by inserting initially a wave perturbation

$$\eta^* = \eta_0 \sin(2\pi(x - x_0)/L) \times \sin(\pi(y - y_s)/(D - y_s)), \quad (2)$$

($\eta^* = 0$ for $y \leqslant y_s$) of the free surface into baroclinic shear flow with a zonal wind profile

$$U = U_0 + U_z z, \quad (3)$$

U_0, U_z constant (z coordinate in the vertical). The initial position of the trough ought to be far to the northwest of the Atlas mountains, so that the formation of a cut-off low near the Atlas mountains may result. Initial winds are in geostrophic balance. Of course, (2) implies that there is a positive anomaly of potential vorticity at the center of the trough.

4. Experiments

In the inviscid experiment A (see Table 1 for a list of experiments) we prescribe a wave (2) with $\eta_0 = -1500$ m, $x_0 = 720$ km, $y_s = 2040$ km, so that the center of the depression is located to the northwest of the Alps (see the star in Fig. 1). The shear is $U_z = 8/\mathrm{D}z = 3 \times 10^{-3}\,s^{-1}$, which corresponds with a temperature difference of $\simeq 40$ K over the width of the channel in the lowest layer. The observed mean meridional temperature

Table 1. *List of experiments discussed more thoroughly in the text*

Experiment	$\eta_0(10^3\ \mathrm{m})$	$U_z(10^{-3}\ \mathrm{s}^{-1})$	Special characteristics	Figures
A	−1.5	3	inviscid	1, 3
A1	−1.5	3	—	—
B	−2	3	—	4, 5, 6, 7
B1	−2	3	westward elongation of barrier	—
C	−2	2.3		8
C1	−2	2.3	westward elongation of barrier	
C2	−2	2.3	large plateau	9

gradient in April is about 8 K/(1000 km) (Fig. 2), so that we assume here a situation of strong but not unrealistic baroclinicity. We witness baroclinic growth of the inserted perturbation with a subsequent cold-air outbreak into the Mediterranean in the rear of the "parent cyclone". After two days the cold air is blocked by the Atlas mountains and is flowing around the eastern and the western ends of the barrier. A depression is forming in the lee of the Atlas mountains. There is also a new cyclone in the lee of the Alps. At $t = 60$ h (Fig. 1) we see a 10 hPa depression in the lee of the Atlas mountains with inflow along the southern flank of the massiv from both sides. However, there is now a ridge to the north of the Atlas mountains. The parent cyclone weakened and moved towards the north. At upper levels, there is a northeast–southwest oriented trough. The southern tip of the trough's axis is located above the Atlas massif. We present in Fig. 3 the variables I, J in the lowest layer. Most of the particles, which were in the channel ($i \geqslant 0$) initially, left the domain to be replaced by particles entering from the west ($i \leqslant 0$). Eastward motion had been particularly fast in the Mediterranean (see also Fig. 1). The most interesting feature is the isoline $I = -30$ in the lee of the Atlas mountains which is not linked to the corresponding isoline to the northwest. This means that the air in the lee must have come from upper levels. Indeed, K-values are relatively large in the lowest layer in

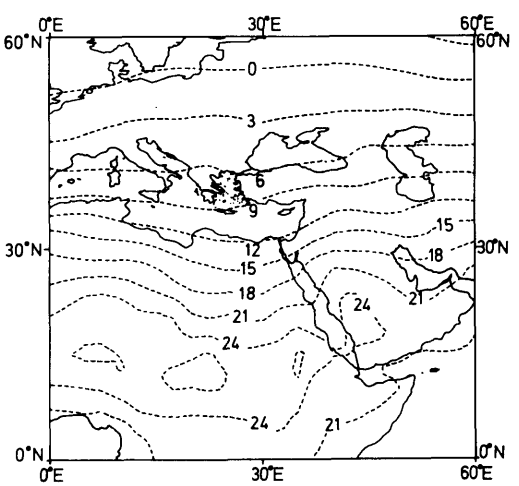

Fig. 2. Mean temperature (°C) at 850 hPa in April in the area of interest; based on a 5-year average over ECMWF analyses.

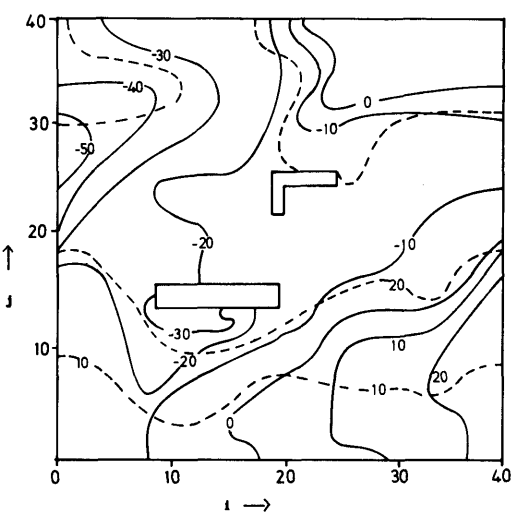

Fig. 3. Lagrangian grid coordinates I (bold) and J (dashed) at $t = 60$ h in experiment A in the lowest layer; i and j give the grid point indices of the model for intercomparison with I and J.

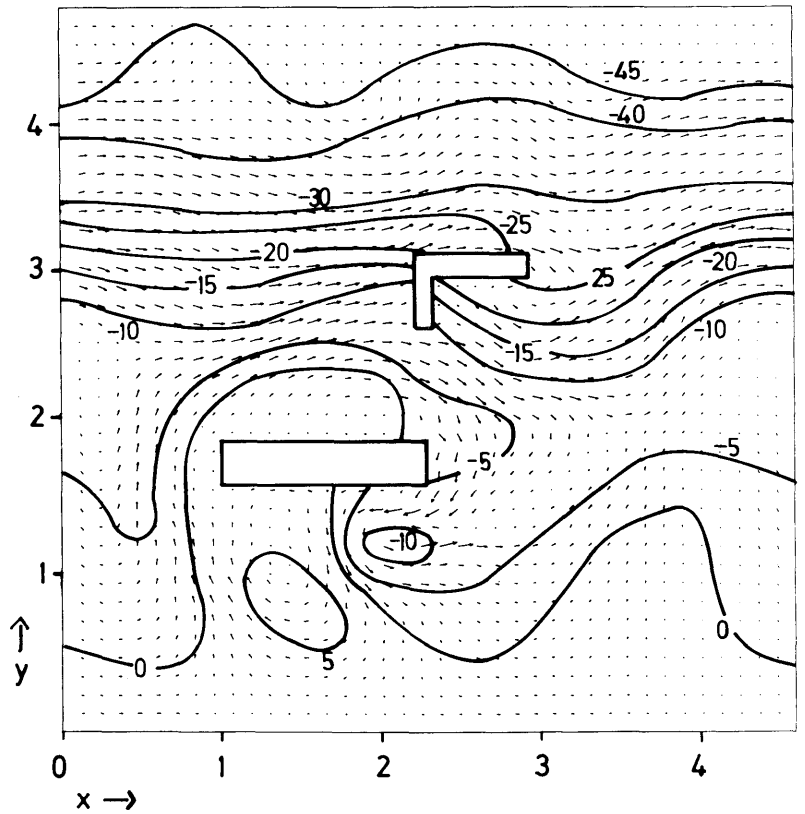

Fig. 4. Wind and deviation pressure (hPa) at $t = 72$ h in experiment B in the lowest layer of the model. Maximum wind speed is 38 ms^{-1}.

this area. The isoline $J = 20$ is located far south in this region because of the cold air outbreak. All this indicates that the Sharav cyclone in Fig. 1 is induced at least partly by the descent of air from upper levels originating far to the northeast of the Atlas mountains. The descent goes with stretching and adiabatic warming. It is partly this air which is seen to flow towards the southeast around the new cyclone. Not surprisingly, no cyclone was found in a parallel run without orography. Instead high pressure is found where the cyclone forms in run A.

Experiment A could not be continued much longer since the numerical quality of the fields began to deteriorate. In an idealized experiment, one would like to be able to exclude friction. In that sense, Fig. 1 demonstrates that friction does not play a role in the formation of the new depression. A viscid parallel run A1 where a damping time of five days is chosen for grid scale diffusion yields maps at $t = 60$ h which are quite similar to

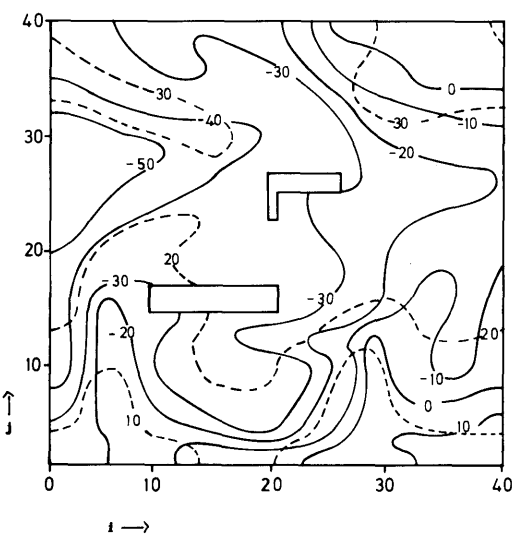

Fig. 5. Lagrangian grid coordinates I (bold) and J (dashed) at $t = 72$ h in experiment B in the lowest layer.

Figs. 1, 3. Experiment A1 has been continued till $t = 96$ h. The new cyclone fills quickly and disappears at about $t = 75$ h. It is unlikely that this filling is due to frictional effects since the new cyclone is quite distinct in experiment A at $t = 60$ h. The frictional time scale is by far too long for such fast evolutions. It is likely that the filling is due to the inflow from east and west along the Atlas wall as seen in Fig. 1. A rather short-lived cyclonic feature evolves to the northeast of the Atlas mountains near the branching point of the southward airflow around the Atlas mountains and the eastward flow to the north. Some indications of this new cyclone can be seen in Fig. 1 already. All in all, experiment A1 appears to capture a case of Sharav genesis where the new cyclone is relatively short-lived and does not move eastward.

In experiment B, an initial increase of the parent's cyclone amplitude to $\eta_0 = -2000$ m is the only change with respect to experiment A1. As before, there is an outbreak of cold air and pressure fall in the lee of the Atlas mountains. The pressure distribution in the lowest layer at $t = 60$ h is rather similar to that in Fig. 1. In particular, there is a cyclone situated at the southern wall of the Atlas massif. As in A1, this low is filling rapidly within the next 12 h. During that time a new cyclone is created to the south of the mountains (Fig. 4) with strong easterly flow to its north in extension of the cold air flow around the eastern end of the barrier and quite pronounced westerly flow to its south similiar to the southwesterly winds in that area in Fig. 1. The (I, J)-map in Fig. 5 indicates that there are strong gradients

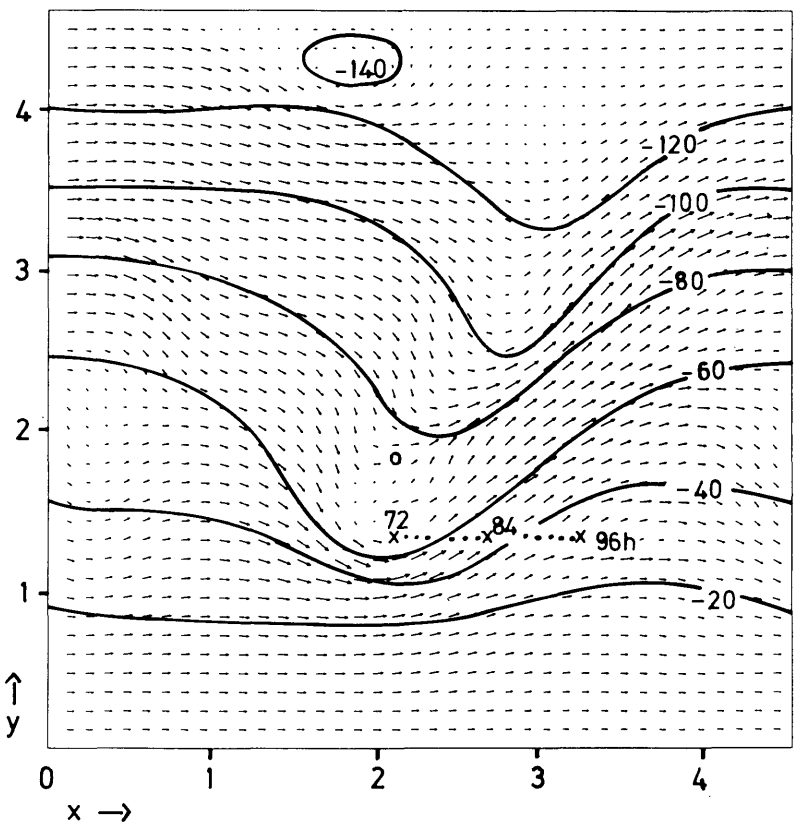

Fig. 6. Wind and deviation pressure (hPa) at $t = 72$ h in the uppermost layer in experiment B (at geometric height $z = 6667$ m). Also given is the position of the center of the Sharav cyclone as evaluated in the lowest layer with a cross every 12 h. Maximum wind speed is 51 ms^{-1}. The small circle indicates the position of a pressure minimum.

of I and J in the cyclone region with cool air from the northwest being located closely to warm air coming from the west. Maximum temperature gradients are more than 5 K/100 km in this area (see also Fig. 7). Although the isoline $I = -30$ in the south of the Atlas mountains is now linked to this isoline in the rest of the domain, it is obvious that the extreme southward extension of this isoline must be due to air stemming from the intermediate level of the model similar to the situation found in experiment A. A parallel experiment B1 has been run to make sure that the eastward flow in the south of the new cyclone originates at upper levels and not from flow around the western end of the Atlas. In B1, we extend the Atlas barrier by about 700 km to the west but choose the same initial state as in experiment B. Flow around the western end of the Atlas cannot reach the cyclogenetic area, but the resulting flow and pressure fields at $t = 72$ h are quite similar to those in Fig. 4. So there is no impact of the western branch of low-level flow around the Atlas mountains on cyclone development in experiment B. At upper levels (Fig. 6) there is a distinct trough with its axis somewhat to the west of the surface cyclone. The cyclone is located on the left side of the jet exit region. One would anticipate cyclone intensification in such a situation. As is seen from Fig. 6 (crosses) the cyclone is moving eastward with a speed of about 14 ms^{-1}. At 84 h (Fig. 7), the new cyclone's circulation is quite vigorous. The cyclone is situated at the western end of a southwest–northeast oriented cold front. Note that there is no pronounced cold front to the west. The upper-level trough is still linked closely to the low-level cyclone. However, there is no doubt that this new

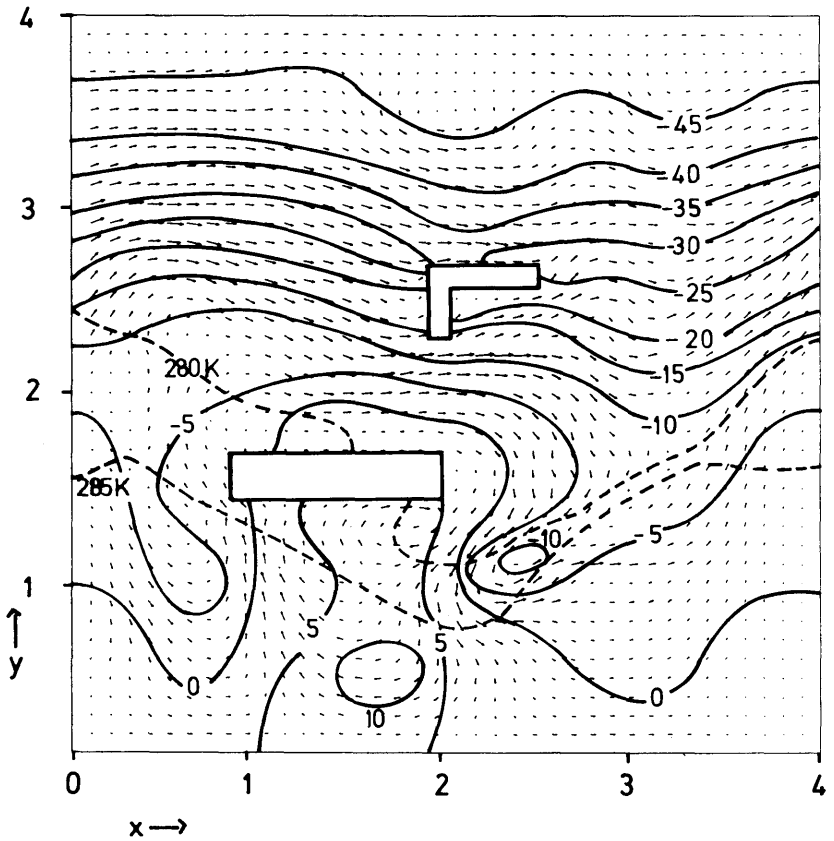

Fig. 7. Deviation pressure (hPa) at $t = 84$ h in experiment B in the lowest layer of the model. Dashed: isentropes $\theta = 285$ K, $\theta = 280$ K. Maximum wind speed is 35 ms^{-1}.

cyclone owes its existence to the Atlas mountains. Cyclone formation does not occur in a parallel run without orography.

Although experiment B appears to suggest that this Sharav cyclone is created by an interaction of orography, upper-level trough and cold front, a third experiment C tells us that the existence of a strong cold front is not a key factor in generating this cyclone. The low-level north–south temperature difference is reduced to 30°C in experiment C, but otherwise we have the same initial state as in experiment B. One has, of course, a reduced speed of the parent's low eastward motion in experiment C and, therefore, the cold-air outbreak reaches the Atlas mountains farther west than in experiment B. The western branch of the low-level flow around the barrier is now quite strong. The upper-level trough crosses the Atlas barrier at its western end and a cut-off low forms. Underneath this cut-off low we find a Sharav cyclone (Fig. 8), which is not linked to a cold front. Therefore, cold front dynamics appears not to be a necessary ingredient in the generation of model Sharav cyclones. In particular, an experiment C1 has been run with an extended barrier (in analogy to B1). In C1, the lee side is almost perfectly shielded from cold-air flow from the north. Nevertheless, a lee cyclone is generated underneath an upper-level cut-off cyclone. Experiments C and C1 make it clear that orographic upper-level cyclogenesis plays a role in our lee cyclogenesis run. This is demonstrated even more clearly in experiment C2, where the elongated Atlas barrier of experiment C1 is extended farther south (dashed rectangle in

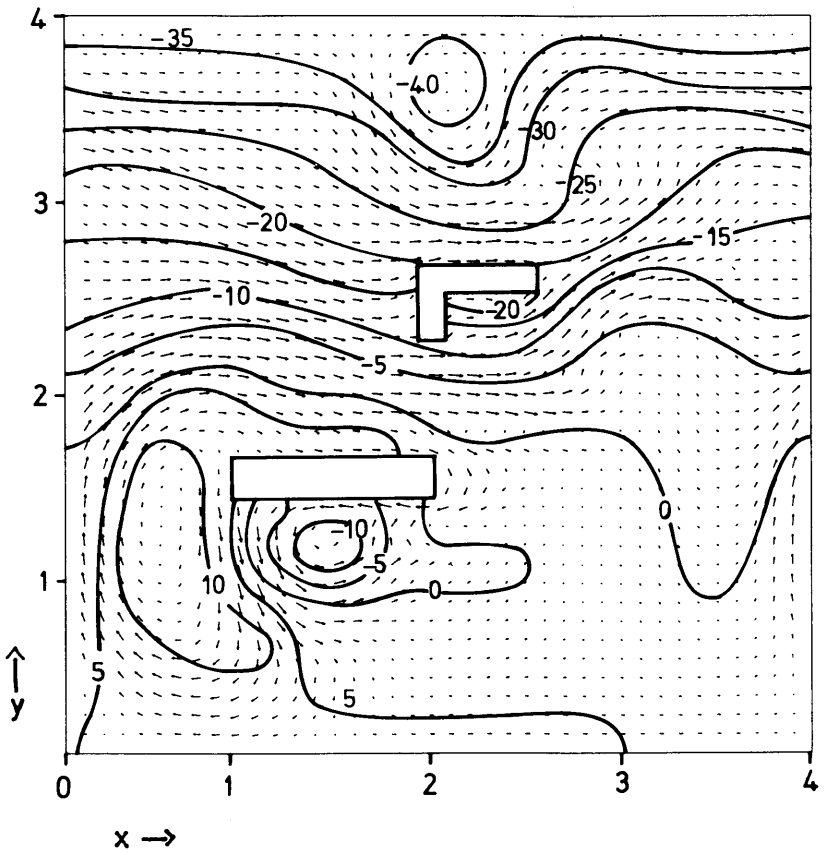

Fig. 8. Deviation pressure (hPa) at $t = 84$ h in experiment C in the lowest layer of the model. Maximum wind speed is 28 ms^{-1}.

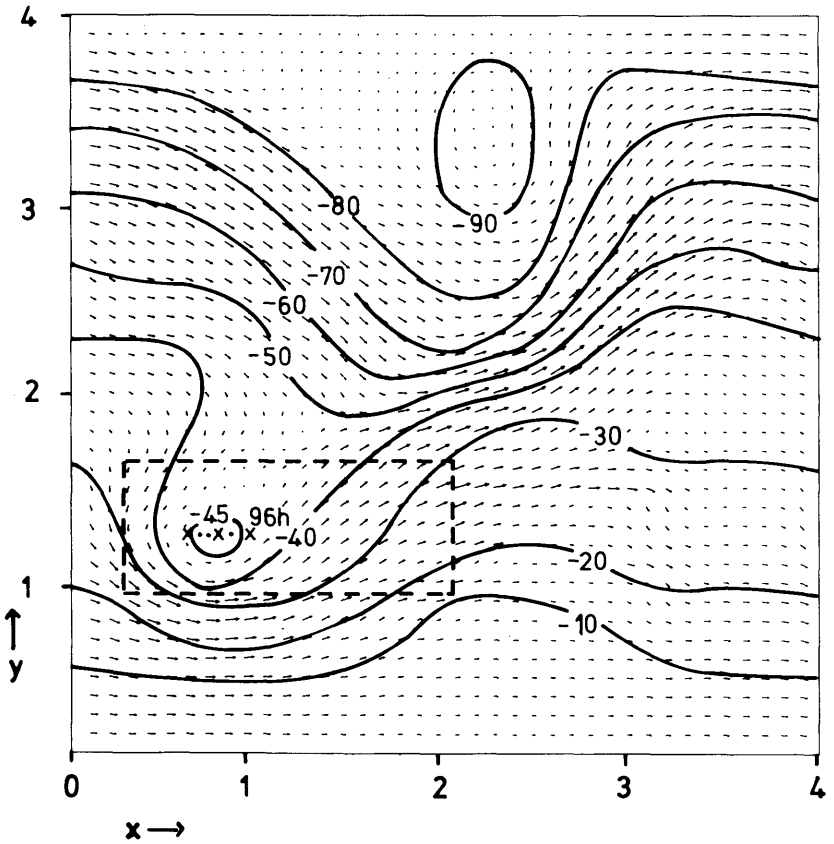

Fig. 9. Deviation pressure (hPa) at $t = 84$ h in experiment C2 in the uppermost layer of the model. Maximum windspeed is 43 ms^{-1}. The size of the enlarged obstacle in the lowest layer is indicated by the dashed lines. The crosses give the position of the pressure minimum at 12 h intervals.

Fig. 9). In that case, a distinct upper-level cyclone forms above the huge plateau. The new cyclone is moving rather slowly and does not deepen till the end of the run at $t = 96$ h. Pressure fall occurs in the lee where a cyclonic circulation is beginning to emerge.

We have conducted several additional experiments to investigate the robustness of the cyclogenesis mechanism as proposed. For example, the wavelength of the incipient low–high system has been reduced to about 3000 km. This did not hinder the formation of the Sharav cyclone. It is the same, if we shift the initial position of the low–high system southward by 900 km. However, there is no cyclone formation if the shift is as large as 1800 km. In that case, the centre of the depression is almost moving over the Atlas mountain, a situation which differs profoundly from that in experiments A–C. Moreover, we concentrated the temperature gradient in the centre of the channel so that a jet is prescribed above the Mediterranean. Again, cyclone formation occurred. Cyclogenesis does not occur if the parent low is too far west initially. Removing the Alps had little impact on the genesis of the Sharav cyclone in a run parallel to experiment C.

5. Discussion and conclusions

In our idealized experiments, we considered a cyclogenesis mechanism which is compatible with the general description given in Weather in the Mediterranean (1962) as quoted in the *Intro-*

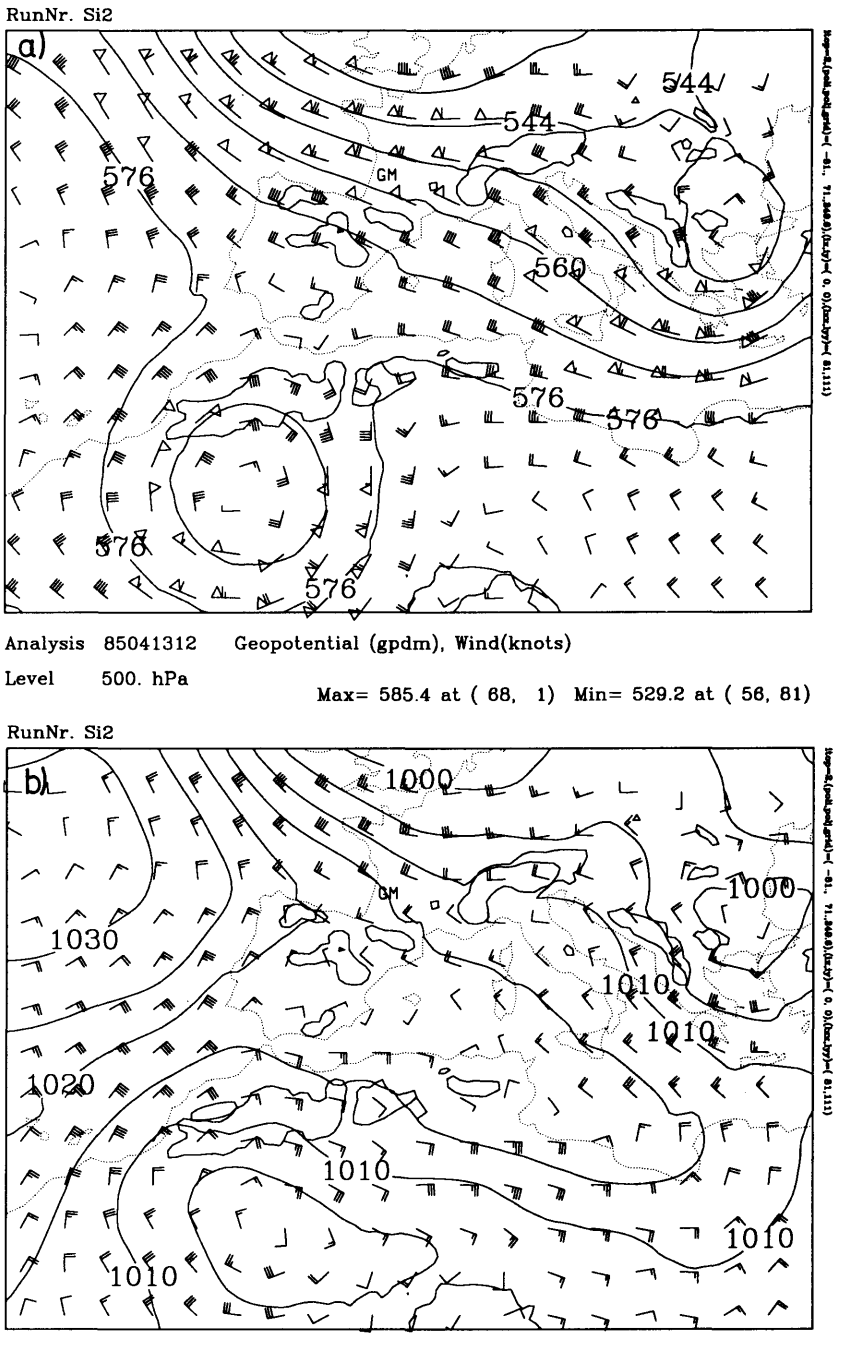

Fig. 10. (a) 500 mb geopotential height (dm) and (b) 1000 hPa height (dashed) and on 15 April 1985. Also given is the wind field. ECMWF initialized analysis.

duction. There is north–westerly wind blowing towards the Atlas mountains and there is a "good supply" of cold air in experiments B, C. We obtain a weak stationary cyclone (experiments A), if the parent low is not of sufficient strength. Unfortunately, as yet no detailed observational analysis of Sharav cyclogenesis has been conducted. Therefore, an intercomparison of observations and model results is difficult. However, we may pick an observed case of Sharav cyclogenesis in order to demonstrate that developments as seen in our charts have counterparts in the atmosphere. To that end we briefly discuss the case of 11–16 April 1985. On 11 April 1985, an upper-level trough moved over the Atlas mountains and a cut-off low is seen on 12 April centered above the lee. A new surface cyclone forms underneath this upper-level flow feature. The lee cyclone is deepening and moving eastward during the next days. We show in Fig. 10 surface pressure, 500 hPa height and winds on 13 April 1985. The new cyclone is slightly ahead of the 500 hPa cut-off cyclone. The similarity of Fig. 10 to our simulations is obvious, except that the model cyclones tend to be located almost exactly underneath the upper-level trough. The similarity is lost to some extent on 15 April, where a new cut-off low forms near the cyclone centre. This intercomparison makes us feel confident that we were able to capture at least one type of Sharav cyclogenesis, where a cold-air outbreak is linked to the southward motion of an upper-level trough. A simulation of this case will be presented in Tafferner et al. (1994).

Finally, we wish to complement the numerical experiments with an admittedly heuristic explanation of lee cyclogenesis as obtained in experiments B–C. To that end we consider a two-dimensional model representing the flow over the Atlas barrier in a north–south oriented crossection (Fig. 11). There are three homogeneous layers, the lowest layer representing the cold air with a surface front at $y = y_F$ underneath an intermediate layer and an upper layer. We assume constant potential vorticity in each layer except for a positive anomaly located in both upper layers, which represents the air near the axis of the upper-level trough. We

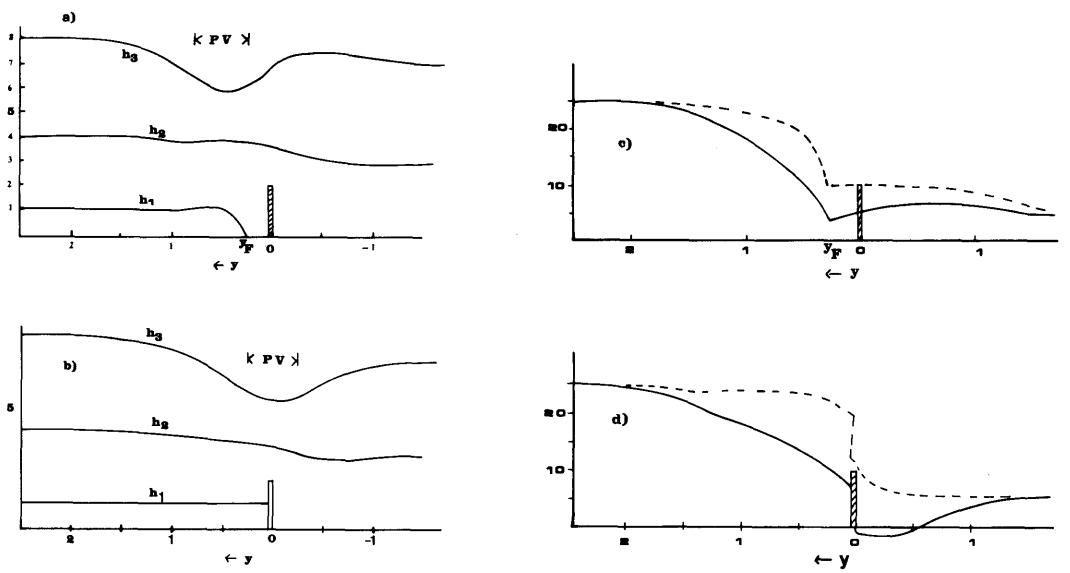

Fig. 11. Conceptual model of the interaction of cold-air blocking and motion of a PV-anomaly over a mountain during lee cyclogenesis. Given are the interface heights (*a*, *b*) and the deviation of surface pressure (*c*, *d*; hPa) from reference value for two situations: in (a), (c) a sinusoidal PV-anomaly is located upstream of the barrier. The horizontal extension of the anomaly is as indicated. The maximum intensity of the anomaly in the uppermost (intermediate) layer is 4.4 (2.2) times that of the background distribution; (b), (d): 12 h later, so that the PV-anomaly is located above the mountain. Also given in (*c*, *d*) is the surface pressure distribution for the case without anomaly (dashed). The anomaly moves almost exactly with the imposed mean wind $V = -10\ \mathrm{ms}^{-1}$. See text for further details.

assume, moreover, that the vorticity is geostrophic. Given the potential vorticity distribution in each layer as well as the position y_F of the surface front, the related height field is obtained by inverting the potential vorticity. Details of this inversion procedure are relegated to the appendix. We assume a superimposed pressure gradient which is balanced by a northerly mean wind $V<0$ in all layers. The motion of the surface front and of the anomalies of potential vorticity are evaluated using a semigeostrophic model. This model is rather similar to that described in Egger and Hatt (1984) and we refrain, therefore, from giving a detailed model description. Moreover, the PV-anomaly moves to a good approximation with speed V as does the surface cold front till it reaches the mountain. After that, the cold air is piling up while the anomaly moves over the mountain.

We consider first a situation where the cold air is to the north of the mountain while the anomaly is situated above the cold air (Fig. 11a). This situation corresponds with the flow after, say, one day in experiments A–C. The upper-level trough linked to the PV-anomaly induces cyclonic vorticity in the cold air. Therefore, the depth of the cold air is increased underneath the upper PV-maximum since the potential vorticity of the cold air is constant. The surface pressure has a minimum at the surface front (Fig. 11c). There is also a minimum linked to the front if the PV-anomaly is removed (Fig. 11c; dashed). Obviously, the PV-anomaly does not induce a cyclone at the ground in this situation. With $V=-10\ \mathrm{ms}^{-1}$ we expect a southward shift of the PV-anomaly by about 450 km within 12 h so that the anomaly is situated partly above the lee at $t=12$ h while the cold air is blocked (Fig. 11b). At that time, a lee "cyclone" is established with a pressure minimum to the south of the barrier. There is no lee cyclone if the PV anomaly is removed.

These idealized experiments demonstrate that it is sufficient for a lee cyclone to form, if the cold air is blocked by the mountain and if a strong PV anomaly moves over the mountain. We feel that this simple explanation captures basic features of what is going on in experiments A–C. However, we have to keep in mind that experiments B, B1 and C, C1 demonstrate clearly that the genesis of Sharav cyclones is a fully three-dimensional process, where air is also flowing around the mountains. Moreover, baroclinic development of the lee cyclone is excluded in our conceptual model. There is no evidence that the same is true in the numerical experiments A–C.

Our idealized experiments demonstrate also that the type of Sharav cyclogenesis considered here shows some similarity to cases of Alpine lee cyclogenesis where cold air blocking and southward motion of upper-level PV-anomalies are known to be important (Tafferner, 1990; Lanzinger, 1992).

6. Acknowledgement

This work has been supported by the German-Israel-Foundation (GIF).

7. Appendix

We consider a three-layer isopycnic model where the density of each layer is ρ_j, constant ($j=1, 3$) and the mean layer thickness is $H_j - H_{j-1}$ ($H_0=0$) for $y \to -\infty$. The orographic profile is $h_B=0$ outside the obstacle, and h_B, constant, in the mountain region. We assume reduced gravity g' in all layers and two-dimensional flow. The height of each interface is h_j. The lowest layer is restricted to the domain $y < y_F$.

The potential vorticity

$$\begin{aligned} P_1 &= f/H_1 + A_1, \\ P_2 &= f/(H_2 - H_1) + A_2, \\ P_3 &= f/(H_3 - H_2) + A_3 \end{aligned} \tag{A1}$$

is given for each layer where anomalies A_i are to be specified. Assuming geostrophic balance for the vorticity in each layer, we may relate all P_i to the heights h_j' via

$$\frac{g'''}{f}\frac{\partial^2}{\partial y^2}h_3 + f = P_3(h_3 - h_2), \tag{A2}$$

$$\frac{1}{f}\frac{\partial^2}{\partial y^2}(g''h_2 + g'''h_3) + f = P_3(h_2 - h_1), \tag{A3}$$

$$\frac{1}{f}\frac{\partial^2}{\partial y^2}(g'h_1 + g''h_2 + g'''h_3) + f = P_1 h_1, \tag{A4}$$

for $y < y_F$ and corresponding equations for the two-layer situation for $y > y_F$. After discretization, the model equations are solved for h_j by relaxation with the boundary conditions for $h_j \to H_j$ for $y \to \infty$, $h_{2,3} \to H_{2,3} - H_1$ for $y \to -\infty$. Moreover $h_1(y_F) = 0$ for $y_F > d$ and $h_1(d) = h_m$ for $y_F = d$ where h_m is the height of the cold air at the northern wall to be prescribed. Note that we do not predict any motions with this model. It is used only to calculate h_i for a given distribution of PV and position of the front. In Fig. 11, we have $g'' = g''' = 0.5\ \mathrm{ms}^{-2}$, $g' = 1\ \mathrm{ms}^{-2}$.

REFERENCES

Alpert, P. and Ziv, B. 1989. The Sharav cyclone: observations and some theoretical considerations. *J. Geophys. Res.* **94**, D15, 18495–18514.

Alpert, P., Neeman, B. and Shay-El, Y. 1990. Intermonthly variability of cyclone tracks in the Mediterranean. *J. Climate* **3**, 1474–1478.

Egger, J. 1988. Alpine lee cyclogenesis: verification of theories. *J. Atmos. Sci.* **45**, 2187–2203.

Egger, J. and Hatt, H. 1994. Passage of a frontal zone over a two-dimensional ridge. *Quart. J. Roy. Met. Soc.*, in press.

Lanzinger, A. 1992. Upper and lower level PV-coupling associated with Alpine lee cyclogenesis. *Met. Zeitschr.* **1**, 173–181.

Mesinger, F. and Pierrehumbert, R. 1986. Alpine lee cyclogenesis: numerical simulation and theory. Scientific Results of the Alpine Experiment. vol. I. *GARP Publication Ser.* **27**, 141–165.

Pedgley, D. 1972. Desert depression over north–east Africa. *Met. Mag.* **101**, 228–243.

Tafferner, A. 1990. Lee cyclogenesis resulting from the combined outbreak of cold air and potential vorticity against the Alps. *Met. Atm. Phys.* **43**, 31–47.

Thorncroft, C. and Hoskins, B. 1991. Frontal cyclogenesis. *J. Atmos. Sci.* **47**, 2317–2336.

Weather in the Mediterranean, 1962. Her Majesty's Stationary Office, London, 2nd edition, vol. 1, 362 pp.